REPORT DOCUMENTATION PAGE

Form Approved OMB No. 0704-0188

1. AGENCY USE ONLY (Leave blank)	2. REPORT DATE	3. REPORT TYPE AND DATES COVERED
	2-June-2000	Final Report

4. TITLE AND SUBTITLE

Investigations into Focused Acoustic Transducers Using Domain Iinverted Materials

5. FUNDING NUMBERS

F61775-98-C0007

6. AUTHOR(S)

Dr Chris Pannell

7. PERFORMING ORGANIZATION NAME(S) AND ADDRESS(ES)

Sensormetrics
29, High Street, Bridge
Canterbury CT4 5JZ
United Kingdom

8. PERFORMING ORGANIZATION REPORT NUMBER

N/A

9. SPONSORING/MONITORING AGENCY NAME(S) AND ADDRESS(ES)

EOARD
PSC 802 BOX 14
FPO 09499-0200

10. SPONSORING/MONITORING AGENCY REPORT NUMBER

SPC 98-4047

11. SUPPLEMENTARY NOTES

12a. DISTRIBUTION/AVAILABILITY STATEMENT

Approved for public release; distribution is unlimited.

12b. DISTRIBUTION CODE

A

13. ABSTRACT (Maximum 200 words)

This report results from a contract tasking Sensormetrics as follows: The contractor will develop and demonstrate an acoustic transducer, approximately 1 centimeter and 0.5 centimeter wide. The transducer will operate at a frequency between 200 and 400 MHz directing the acoustic beam by means of a technique equivalent to a fresnel zone plate into a line focus at a nominal distance 0.5 cm from the transducer and lying at an angle of 3 degrees to the plane of the transducer. The primary objective is the production and demonstration of a device in which a domain inverted acoustic transducer is bonded to a suitable substrate used to produce an intense acoustic field in the form approximating to a line focus, and to facilitate the attachment of an optical fiber at this position.

14. SUBJECT TERMS

EOARD, Fibre Optics, Acoustics, Optical fiber sensors, Optical communications

15. NUMBER OF PAGES

34

16. PRICE CODE

N/A

17. SECURITY CLASSIFICATION OF REPORT	18. SECURITY CLASSIFICATION OF THIS PAGE	19, SECURITY CLASSIFICATION OF ABSTRACT	20. LIMITATION OF ABSTRACT
UNCLASSIFIED	UNCLASSIFIED	UNCLASSIFIED	UL

NSN 7540-01-280-5500

Standard Form 298 (Rev. 2-89)
Prescribed by ANSI Std. 239-18
298-102

Air Force Office of Scientific Research contract number SPC-98-4047, Entitled:

"Investigations into focused acoustic transducers using domain inverted materials"

Starting date July 10_{th} 1998

Final report, March 2000, Item 0003

Prepared by:

C N Pannell
57, New House Lane
Canterbury
Kent CT4 7BJ, UK.
Tel: (+44) 1227 463022
Email cnp@orange.u-net.com

Harald Gnewuch
Physics Building
University of Kent
Canterbury
Kent CT2 7NR

Liam Humberstone
Physics Building
University of Kent
Canterbury
Kent CT2 7NR

On behalf of:

Sensormetrics Ltd,
29, High St, Bridge,
Canterbury,
Kent, CT4 5JZ, UK.
Tel: (+44) 1227 831076
Fax (+44) 1227 831991

Proposal initiated by:

Dr Paul Szczepanek,
Chief, Solid State Physics Branch,
Laboratory for Physical Sciences,
8050, Greenmead Drive,
College Park, MD 20740.
Tel: (301) 935 6535
Fax: (301) 935 6723
Email: pss@lps.umd.edu

Contents

1. Background and overall objectives

1.1 Initial design

The principal objective of this project is the development of an acoustic modulator which functions by causing coupling from optical fibre guided modes to cladding modes when acoustic energy is supplied. The device consists of an acoustic transducer bonded to a suitable substrate capable of producing an intense acoustic field in the form of a line focus approximately 1 cm in length. An optical fibre will be positioned at the line focus, and tilted slightly with respect to the focal line for the application required. Dr Szczepanek has stated that he would like specific values of acoustic frequency/tilt angle and has given two possible acceptable combinations as:

(a)	**frequency**	**= 196 MHz**	**(b)**	**freqency**	**= 150 MHz**
	angle	**= 3.15 deg**		**angle**	**= 4.11 deg**

with option (a) being preferred as being more efficient.

1.2 Transducer alternatives

As indicated in the original proposal the material of choice for domain inverted acoustic transducers is barium sodium niobate, often referred to as BSN. This is because the electromechanical constant of the z-cut material operating as a thickness mode transducer is exceptionally high, in fact it is 0.57 compared to the z-cut of lithium niobate (0.17) and the 36^{O}-rotated y-cut of lithium niobate (0.49) usually used to generate bulk longitudinal acoustic waves. We tried to locate sources of BSN throughout the project but have been unable to find a suitable source. We know that the material can be sputtered so as to form thin-film acoustic transducers, and we have obtained some targets of the sintered material, but on reading the literature we expect RF sputtered BSN to be a problematic material, and worthy of a study in its own right. Because we have a PhD student for 3 years, we will carry this work on if necessary after the official end of this project.

Compared to sputtered Zinc Oxide, with an electromechanical coupling constant of 0.28, close to the single crystal value, BSN would appear to offer advantages assuming that the electromechanical coupling constant of the sputtered films is also close to the single crystal value. BSN can be domain inverted, and so if it can be deposited reproducibly, it will be a very versatile material for advanced transducer design.

In order to stay on track, and because of the uncertainties in depositing and poling BSN, we have decided to work with commercially available $LiNbO_3$. One other major advantage of this material is that we anticipate that the device will need to be supplied with the order of 1 Watt of RF power, and although single-crystal $LiNbO_3$ is known to be capable of handling the power, initial experiments performed by us and by others tend to suggest that are that sputtered films of ZnO (and this is probably true of BSN) tend to undergo irreversible damage at high RF powers.

1.3 Form of the focal region

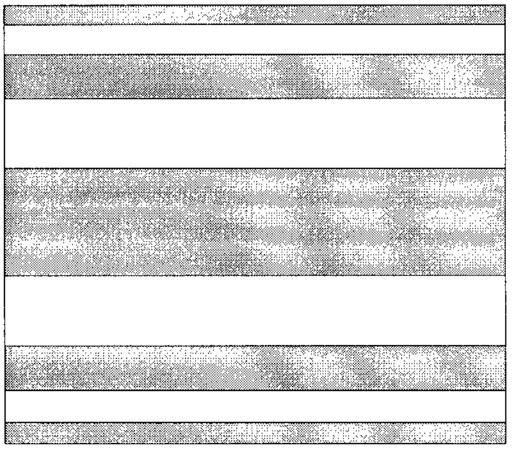

Figure 1.1: Schematic of domain inverted transducer suitable for producing focused cylindrical waves.

In order to produce a cylindrical focus, the domain inverted acoustic transducer will be in the form of parallel stripes of alternating polarity, the arrangement being symmetrical about the (widest) central stripe, see figure 1.1.
This particular transducer contains 5 domain inverted stripes, shown shaded.
The arrangement acts as a "Fresnel zone source" with the widths and positions of the various stripes arranged so that there is constructive interference at the desired focus, as shown in figure 1.2.

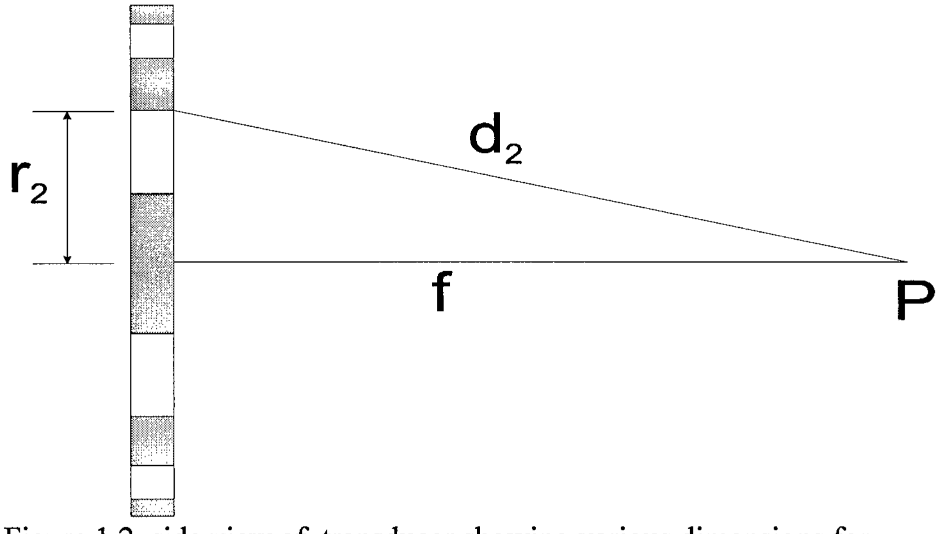

Figure 1.2, side view of transducer showing various dimensions for producing a line focus normal to the paper and through P.

The latter condition yields the following formula for successive positions of the boundaries between the domain inverted regions

$$r_n = \sqrt{\frac{(2n-1)\lambda}{2}\left\{f + \frac{(2n-1)\lambda}{8}\right\}} \quad , \quad n = 1,2,3... \qquad (1.1)$$

1.3.1 The relationship of the form of the focal region to the number of stripes in the transducer.

If the transverse co-ordinate x in the focal region is measured from the axis of symmetry, the amplitude distribution in the transverse plane a distance f from the array is given to reasonable accuracy by the simple 1-D Fraunhofer diffraction integral

$$U(x) = \frac{\exp\{i\phi\}}{i\lambda f} \int_{-\infty}^{\infty} U(x) \exp\left\{ -\frac{i2\pi\, x x_1}{\lambda f} \right\} dx_1 \qquad (1.2)$$

In equation (2), ϕ is a phase factor which is unimportant for our present purposes, as we are only interested in the intensity in the focal region here. Also, for our present purposes it is sufficient to consider U as having only two values, +1 and -1, corresponding to the un-inverted and inverted regions respectively. The positions at which the switch from +1 to -1 or vice versa occurs is given by the values of r_n defined in equation (1.1). We can normalise U by dividing by the U obtained with a single stripe of half-width r_1, where r_1 is defined by (1). When this is done for a $LiNbO_3$ transducer having n=15, taking f=196 MHz, and picking a focal length of 4 mm, we get by integrating equation (2) and taking the modulus squared, the peaked curve shown in figure (1.3).

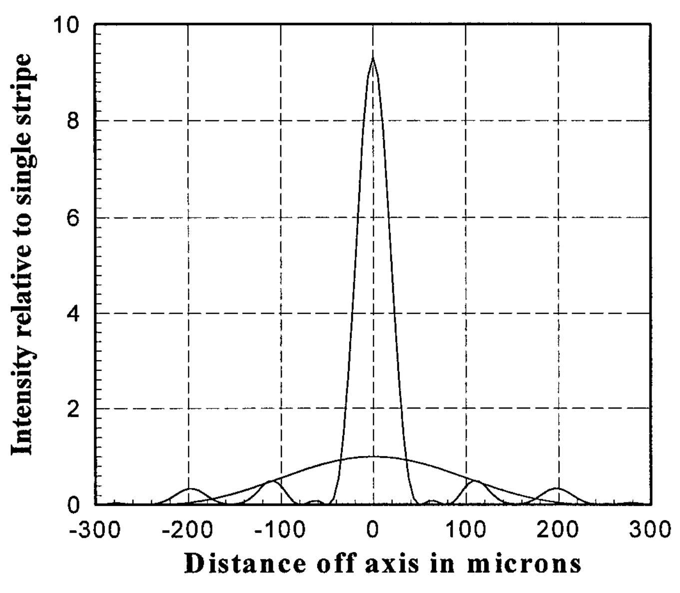

Figure 1.3: Curves showing relative intensities for n=1 and n=15 domain inverted $LiNbO_3$ transducers. The total width of the n=1 stripe is 0.493 mm, the total width of the n=15 array is 2.692 mm. The focal length is 4 mm

We are assuming a longitudinal acoustic velocity of 5.96×10^3 ms^{-1}, the acoustic wavelength is 30.4 μm.

We can therefore see from figure 1.3 that the acoustic intensity is approximately nine times higher than if a single stripe electrode corresponding to the central part is used. Figure 1.3 also shows that the full width half maximum (FWHM) of the focal region is of the order of 50 μm, which gives a measure of the mechanical tolerances which need to be achieved in the process of alignment.

A shorter focal length would decrease the transducer width, which would be good from the point of view of increasing the radiation resistance and making it easier to match electrically, however the disadvantage is the operating at lower f-numbers means that the device is more prone to acoustic aberrations and this "blurs" the acoustic focus.

1.4 Substrate alternatives

We have considered different substrate materials, principally aluminium and the borosilicate glass BK7.

Connecting more than two transducers in series is difficult if the substrate is metallic, as electrically floating electrodes are needed. This could be advantageous for example because the radiation resistance of a single transducer of the area required here can be low compared to 50Ω making electrical matching difficult. Several options are available if the substrate is dielectric, including the use of patterned back electrodes and epoxy bonds, or the use of indium bonding followed by cutting of narrow slots through the transducer/bonding layer to isolate the bottom electrodes electrically from each other.

Advantages of using aluminium substrates for this work are:

(i) The metallic substrate is a much more effective heat sink than silica, useful for high power applications such as this.

(ii) We know from previous experience that the aluminium can be embossed by means of a suitable steel wire pressed into it so as to give an excellent Hertzian contact with an optical fibre. If for example a straight stainless steel wire of ~127 μm is compressed between a pair of identical flat aluminium plates, a pair of "U-grooves" are formed which are, on relaxation, ~125 μm in diameter. The best that can be done with a silica substrate is to cut a rectangular or V-shaped slot, put in the fibre and use a material such as epoxy as a filler. The use of epoxy at these frequencies in layers more than a couple of microns thick is almost certainly likely to result in large acoustic loss and therefore unwanted heating.

If we want both the freedom to be able connect transducers in series (dielectric substrate) and retain the heat sinking/ U-groove technology (aluminium substrate) to hold our fibres, we could consider a structure consisting of a BK7 plate a few mm thick, with the transducer array bonded on one side and an aluminium plate carrying the U-groove on the other. Indium or epoxy bonding could then be used throughout with the advantage that no filler materials are required.

Table 1.1 shows some of the relevant mechanical properties of BK7 and aluminium. It can be seen that the specific acoustic impedances for aluminium and BK7 are very similar, an advantage for the "compound" structures proposed here.

material	Longitudinal Velocity $ms^{-1} \times 10^3$	Specific Acoustic impedance $kgm^2s \times 10^6$	Acoustic attenuation $dBs^2m^{-1} \times 10^{-15}$
aluminium	6.42	17.33	0.355
BK7	5.96	13.1	0.17

Table 1.1: Properties of substrate materials

The main advantage of using a substrate of glassy material such as BK7 is that it makes alignment of the transducer with the optical fibre much easier. As the project progressed, we realised that this is the critical step, and so we finally decided to use BK7, with a system of alignment marks etched onto the substrate and the transducers to facilitate alignment.

1.5 Transducer bonding alternatives

The main alternatives considered for this project were :

(i) Indium compression bonding
(ii) Epoxy bonding
(iii) Bonding using polyimide resin

Certainly (i) is the most efficient and robust bond, but the main problem is the alignment of the transducer focal line with the fibre inside the vacuum chamber. Of course, one could imagine bonding the transducer first and then using some technique to locate the focal line, perhaps using a fibre-optic vibrometer to examine the surface displacement of the substrate, but this was ruled out as being too complicated and rather indirect. Again we would rather use a transparent material for the bond, in order to be able to use a system of alignment marks for final assembly.

We considered polyimide, and performed some experiments spinning onto a substrate, but the material requires high curing temperatures, and although it is known to have a high Youngs modulus, it is poorly characterised in terms of acoustic impedance and more importantly, acoustic loss. Thus we were led to consider epoxy as a bond material.

Because epoxy type materials are likely to be used in the device described here, we need an idea of the effect of this material on transmitted and absorbed acoustic powers.

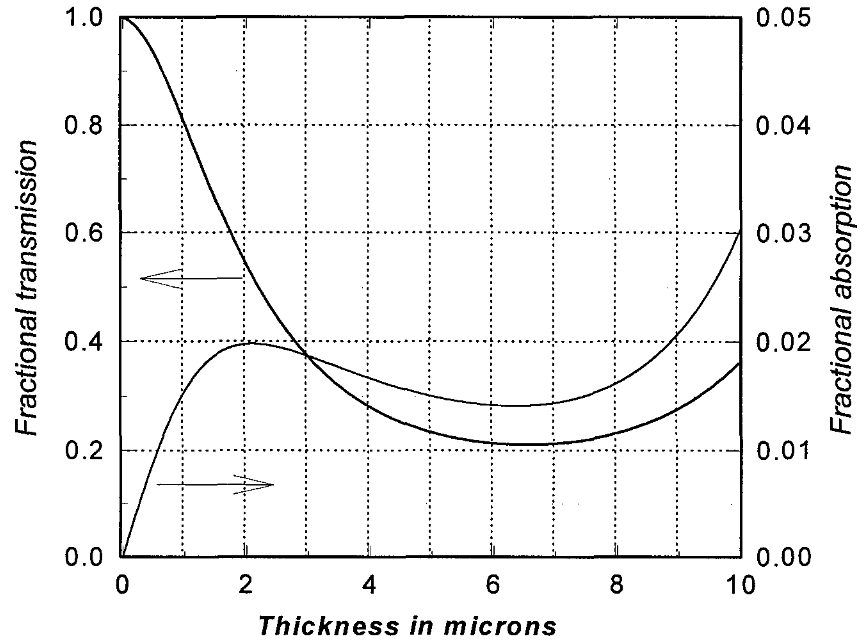

Figure 1.4: Absorbed and transmitted acoustic power at 196 MHz for a thin layer of epoxy sandwiched between two layers of silica

From figure 1.4 we can see that for epoxy layers of thickness less than approximately 1.5 μm, the effects are not particularly serious, either in terms of absorbed acoustic energy or reflections. More than 70% of incident acoustic power will be transmitted, and ~1.8% will be absorbed. The rest will be reflected. For plotting this graph we have taken the acoustic losses as 0.2dB μm^{-1} GHz^{-2}.

2 Alternative methods of production

In this section we describe the various techniques we have tried for making the substrate and for fixing an optical fibre into it with a good quality acoustic joint.

2.1 Wedged plates

We first examined the possibility of using a simple wedged plate for the substrate, with the optical fibre fixed into a groove on one side and the transducer bonded to the opposite side. This was dismissed for the present, as there are several major problems.

The first problem involves the process of fixing the transducer onto the substrate, this will involve some form of compression bonding technique (see section 4), and parallel surfaces are advantageous if this operation is to be carried out without cracking the transducer. It is possible that we could obtain wedged blocks and using an identical "dummy" block underneath it, arrange for the total thickness to be constant, but this was thought to be too complicated and has not been tried yet. We do plan to continue experiments on this, and will try later, also using the groove pressing technology we have developed, see section 2. It was decided, however, to construct a prototype using an accurately cut parallel sided block of BK7 with a groove machined using a precision dicing saw.

2.2 Fibre grooves

The ability to make a good acoustic contact between the optical fibre and the substrate is of vital importance in this type of device, and we have been investigating several possibilities. We have decided to investigate three main techniques, sawing, etching and hot-pressing of wires.

The ability to make U-shaped grooves in soft metals such as aluminium using wires, is a very attractive reason for basing this device on an aluminium substrate. However, the small transducer thickness required for the specified frequency of operation (~20 μm), together with the thinness of the plate (~4mm) means that the transducer will be liable to breakage, either by forces transmitted to the transducer during bonding of the fibre, or by the effects of differences in thermal expansion.

Another reason for preferring a non-metallic substrate is that in order to increase the impedance of the domain inverted transducers to the point where electrical matching is relatively easy, one or more electrically floating bottom electrodes are required, this cannot easily be done when the substrate is metal.

As explained in section 1.4 we have decided to use BK7 glass for the device substrate. It is capable of being polished easily to the 60/40 finish commonly regarded as necessary in the acousto-optic industry for transducer bonding, while aluminium alloys are rather marginal in this respect. The mismatch in acoustic impedances is very small, the specific acoustic impedances (longitudinal) for BK7 and silica are both 13.1×10^6 $kgm^{-2}s^{-1}$.

We have been investigating the means by which we can make a U-groove in this material, with the object of bonding a fibre into it with very little "filler material" being necessary.

2.2.1 Etching grooves

We first investigated the use of HF to etch grooves in BK7. We used photolithography to mask off the substrate which is not to be etched and define the extent of the groove. Rather surprisingly perhaps, our experiments have revealed that we could use ordinary photoresist to do this job. Figures 2.1-2.5 show the results of some preliminary experiments with plates of BK7 glass.

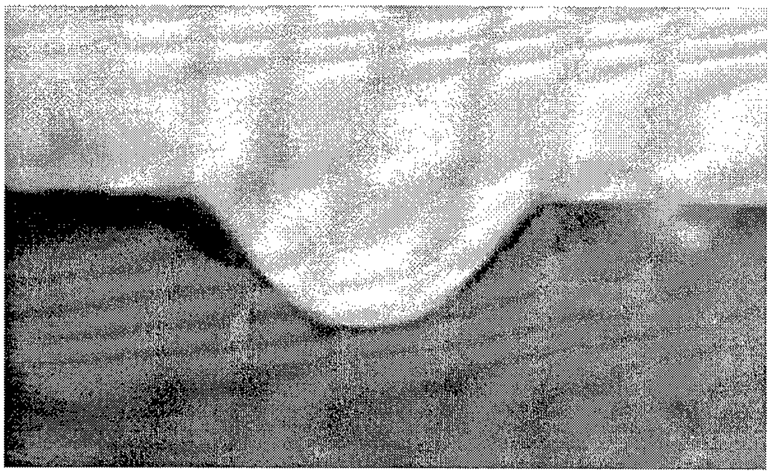

Figure 2.1: Side view of BK7 plate after 2 hour etch at room temperature, groove depth is 11μm, photoresist opening 1.5 μm wide.

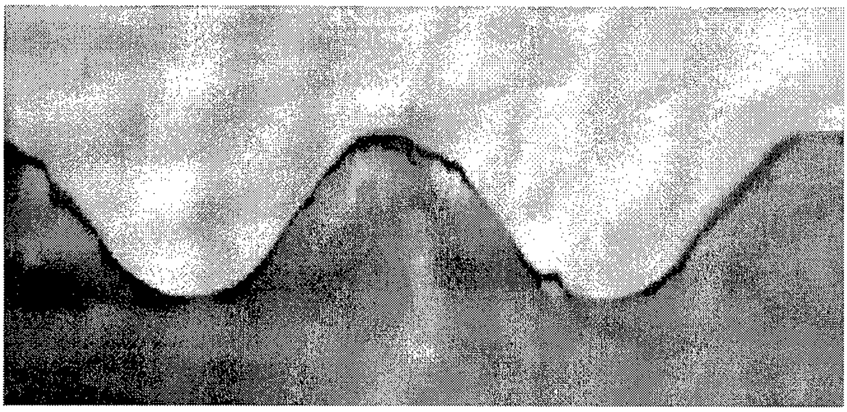

Figure 2.2: Side view of BK7 plate after 5 hour etch at room temperature, groove depth is 29μm, photoresist opening 1.5 μm wide.

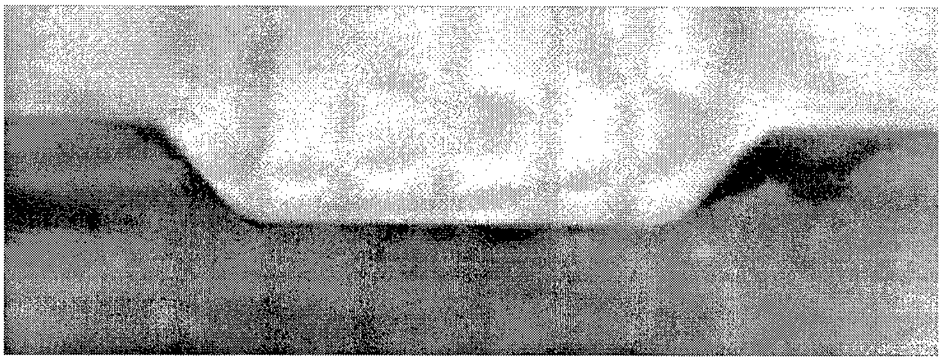

Figure 2.3: Side view of BK7 plate after 2 hour etch through 50 μm opening, room temperature

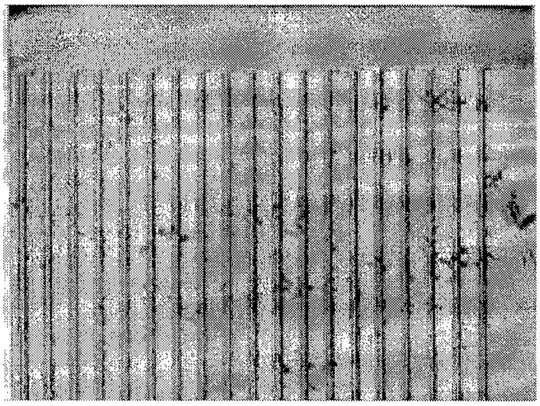

Figure 2.4: Top view of 50 μm openings

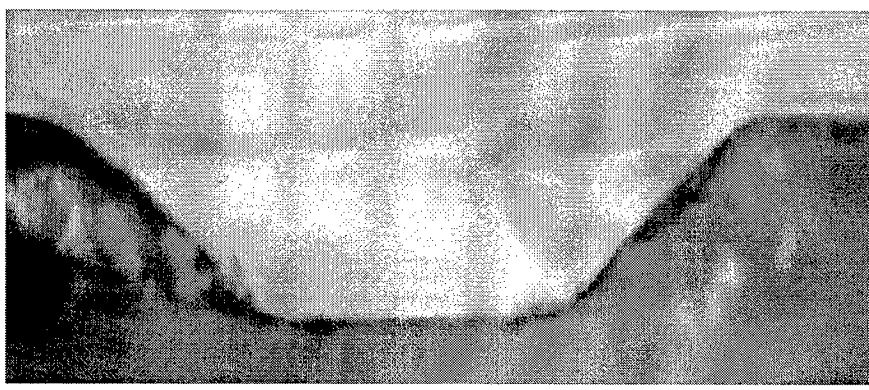

Figure 2.5: Side view of BK7 plate after a 5 hour etch through a 50 μm opening, room temperature

It can be seen from the figures that a suitable groove can be produced by this method. The important factor is the angular range over which good contact between the fibre and the groove is maintained. With a device having a focal length f=3.5 mm, with a transducer of width w = 2.7mm, the angle over which contact needs to be maintained is just $2\tan^{-1}(w/f) = 42^{O}$. From the experiments, we measured a suitable radial curvature over 100^{O} for a 2 hour etch and 84^{O} for a 5 hour etch. Linear extrapolation shows that 54 degrees of good contact can be expected with a groove width of 125 μm, the conclusion is therefore that etching can give grooves of the required properties, although etching times substantially longer than 5 hours will be needed.

2.2.2 Pressing grooves

Encouraged by our results pressing steel wires into aluminium blocks, we decided to try the same idea on some test samples of BK7 in the form of discs. We have built a device in which a stainless steel wire under slight tension (and therefore held straight) initially lying flat on the BK7 test disc is pressed into it at elevated temperatures by means of a hydraulic ram. The apparatus is shown in figure 2.6.

The abbreviations are as follows :

TC = thermocouple
BS = Borosilicate, i.e BK7 glass
R = Rod with groove for wire alignment
M = Macor (machinable glass ceramic)
W=wire

D = Duratec 750
TF = tube furnace
S = stainless, high temperature steel (303)
B = base

Tests on this have now been carried out. We needed to empirically determine the temperature at which the viscosity of the glass had fallen to a value which allows pressing in a convenient time, and at a force which will not cause shattering. A suitable vertically mounted tube furnace/hydraulic ram is available and was used in these experiments. An alternative method might be to press the wire into the surface while passing an electrical current through it to heat it to the required temperature. This would remove the need to heat the entire assembly up, and would be useful if the transducer was already bonded when the groove was pressed.

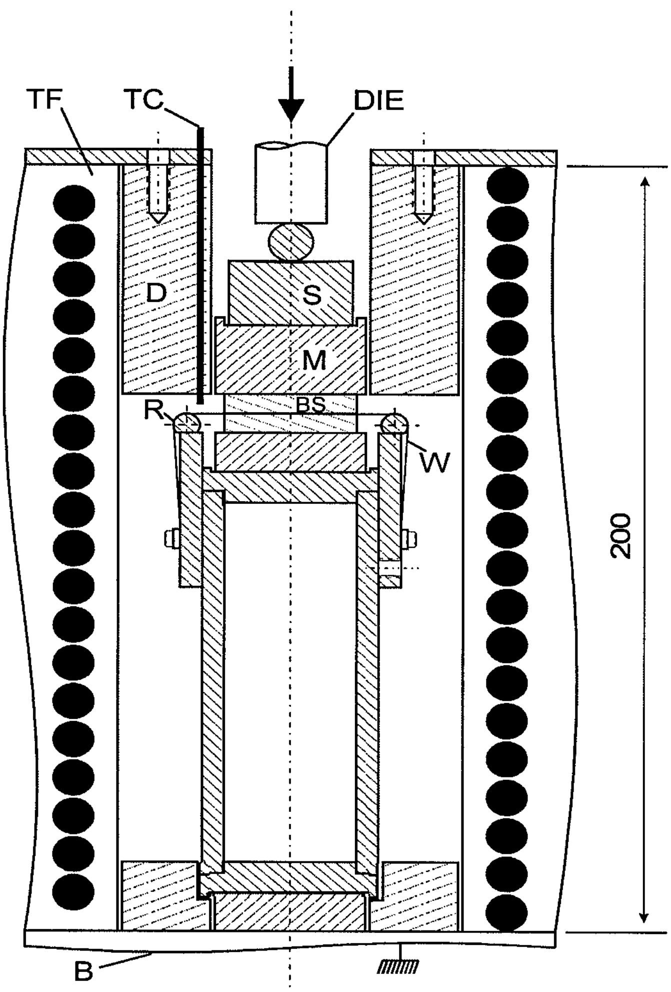

Figure 2.6 Schematic of the U-groove-pressing jig.

Figure 2.7 shows the result of pressing a 125 μm wire into a plate of BK7 at a temperature of $600^{O}C$, after cutting the glass substrate. It can be seen that the form of the lower part of the groove is an excellent fit to an optical fibre, as is to be expected. We feel that this technique has important applications for the construction of various fibre-optic devices, as it provides a means of mounting an optical fibre in a dielectric material of similar mechanical properties (principally thermal expansion coefficient) with the minimum of "filler". If a single stainless steel wire is pressed between an identical pair of such flat plates, then we have a situation in which the groove is such that the fibre axis is level with the surface.

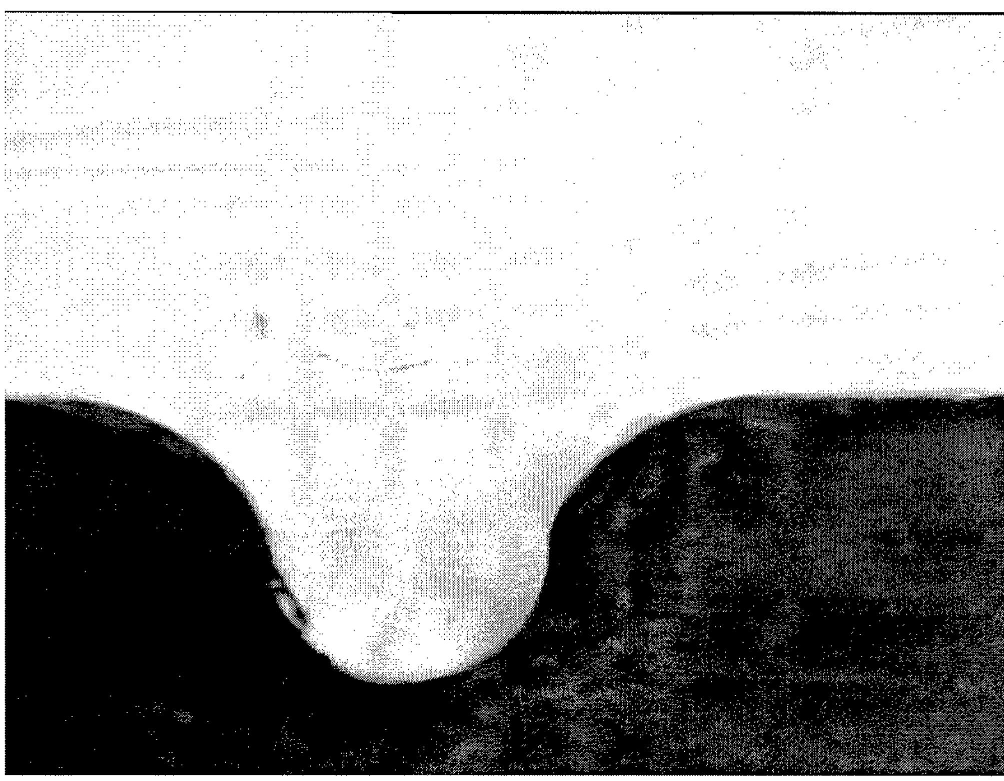

Figure 2.7: Side view of BK7 plate after a tensioned stainless steel wire of diameter 125 μm is pressed in at a temperature of $600^{O}C$ with the apparatus of figure 2.6.

The device of figure 2.6 was mounted on the bed of a 30 tonne hydraulic press of the type used in garages for inserting cylinder linings etc, the hydraulic ram pressed down into a vertically mounted tube furnace which was capable of being ramped up to the desired temperature over a period of time, and then after a period at the desired temperature, ramped back down to room temperature.

2.3 Cutting grooves with a dicing saw.

Using a dicing saw fitted with a blade of suitable thickness and matrix, a groove, inclined to the correct angle for the respective device, is cut into the glass block. In order to achieve the required angle for the amplitude modulator, the blocks are waxed onto a stainless steel block that has been machined into a suitable wedge. This approach gives good control of the angle and as will become apparent, facilitates the alignment method that is used for the transducers.

During our work on groove production we noted our assumption that diamond grit size correlating to surface finish was incorrect. Small grit sizes tend to clog with glass very easily, resulting in blades overheating and then breaking. Larger grit sizes actually break down sufficiently quickly to expose a fresh cutting edge, ensuring the required surface finish is attained. This method does not ensure the bottom of the groove is semi-circular in profile, but we believe that using Indium soldering techniques to bond the fibre into the groove means that this problem is of little consequence. We have found that it is possible to "dress" the blades in such a way that they are able to cut a semi-circular groove in the substrate, but as yet we have not managed to do this reproducibly.

We found the optimum cutting parameters to be:

3" resin bonded blade at 30,000 rpm

Feed rate - 8 mm/s, down cut only

325 mesh grit size

Direct water cooling

2.4 Conclusions

We have experimented with three techniques for the purpose of making grooves in our glass substrates, which will be a reasonably close fit to our (round) optical fibre, and therfore have the potential to form a good acoustic and mechanical joint. We tried etching, pressing and cutting with a dicing saw. We found the pressing to be very interesting and more work will be done to exploit the technique during the remaining period of study of the PhD student working on the project, Mr Liam Humberstone. We decided to use the third method, involving the dicing saw, as we can easily produce the angled grooves needed for this project, while retaining the two flat and parallel surfaces of the substrate block, important for transducer bonding. Again, we feel that transducers could be bonded to wedged substrates, but that the degree of uncertainty introduced into the project is unacceptable for the prototype. We will continue this work.

Grooves cut with a dicing saw tend to be rectangular in cross-section, but this is not very important as the gap between the cylindrical surface of the fibre and the flat surface at the bottom of the groove is small over the angular subtense of the incident acoustic beam. We will use indium soldering to fix the (aluminium jacketed) fibre into the groove to minimise any acoustic mismatch problems.

3 Detailed considerations of transducer manufacture

In this section we describe the process steps necessary for the transducer manufacture, the photolithographic mask layout, experimental poling details and results, followed by conclusions.

3.1 Process steps of transducer manufacture

The transducers have been manufactured using the following order of process steps :

- *Wafer dicing :*
  300 μm thick z-cut $LiNbO_3$ wafers where diced parallel to the x- and y-crystal axis. The area of the cut samples was (11x18) mm^2 , which is determined by the transducer area plus a margin of 4 mm width around that area to avoid electric breakdown during the poling process.
- *Cleaning of diced wafer samples.*
- *Alignment mark patterning :*
  Positive photoresist spun onto the $-z$-face was patterned photolithographically.
  The photolithographic mask was positioned with respect to two orthogonal edges of the $LiNbO_3$-sample, thus guaranteeing both a greater than 4 mm margin around the area to be poled and the parallelism to the x- and y-crystal axis.
- *Alignment mark etching :*
  The alignment marks were dry etched using a Reactive Ion Beam Etcher (RIBE) to a depth of approx. 250 nm.
- *Cleaning, photoresist deposition and poling-area patterning :*
  The samples underwent a very thorough cleaning procedure in order to avoid surface current leakage through contaminants (mainly water) and thus to guarantee perfect electric insulation by the patterned photoresist between mask openings. Cleaning and drying of the samples was immediately followed by spin-coating of photoresist on the $-z$-face. The samples were then soft-baked and left for a while to electrically discharge. The photolithographic patterning of the photoresist for the poling process was done with respect to the etched alignment marks. The photolithography was done with great care to ensure very sharp and uniform corners – nucleation points of the domain inversion - formed by the photoresist and the sample surface.
- ***Further preparation of samples for domain inversion :***
  Prior to domain inversion the 4 mm wide margin around the sample was covered with insulating tape.
- *Domain inversion by electric field poling* . The poling process and the results obtained are described in detail in other sections below.
- *Cleaning.*
- Cutting off the 'poling margins' around the partially domain inverted areas and alignment marks in order to fit onto the glass blocks.
- *Very thorough cleaning.*
- *Chrome-gold coating on the $-z$-face by thermal evaporation.*
- *Photolithographic patterning of photoresist on the $-z$-face for 'bottom' electrode, aligned with respect to etched alignment marks.*
- *Chemical wet-etching of chrome-gold.*
- *Removal of resist $\Rightarrow$ ready for bonding.*

3.2 Mask layout details

Figure 3.1 shows the mask layout of the photolithographic 'dark-field' mask used for all photolithographic processes necessary for device fabrication. The functional segments of the mask a numbered and their use explained in Table 3.1. In addition to the photolithographic processes described above the mask also contains segments for the patterning of the 'top electrode', which is two-segmented, and for the etching of alignment marks in the glass which themselves are aligned with respect to the sawed or pressed groove.

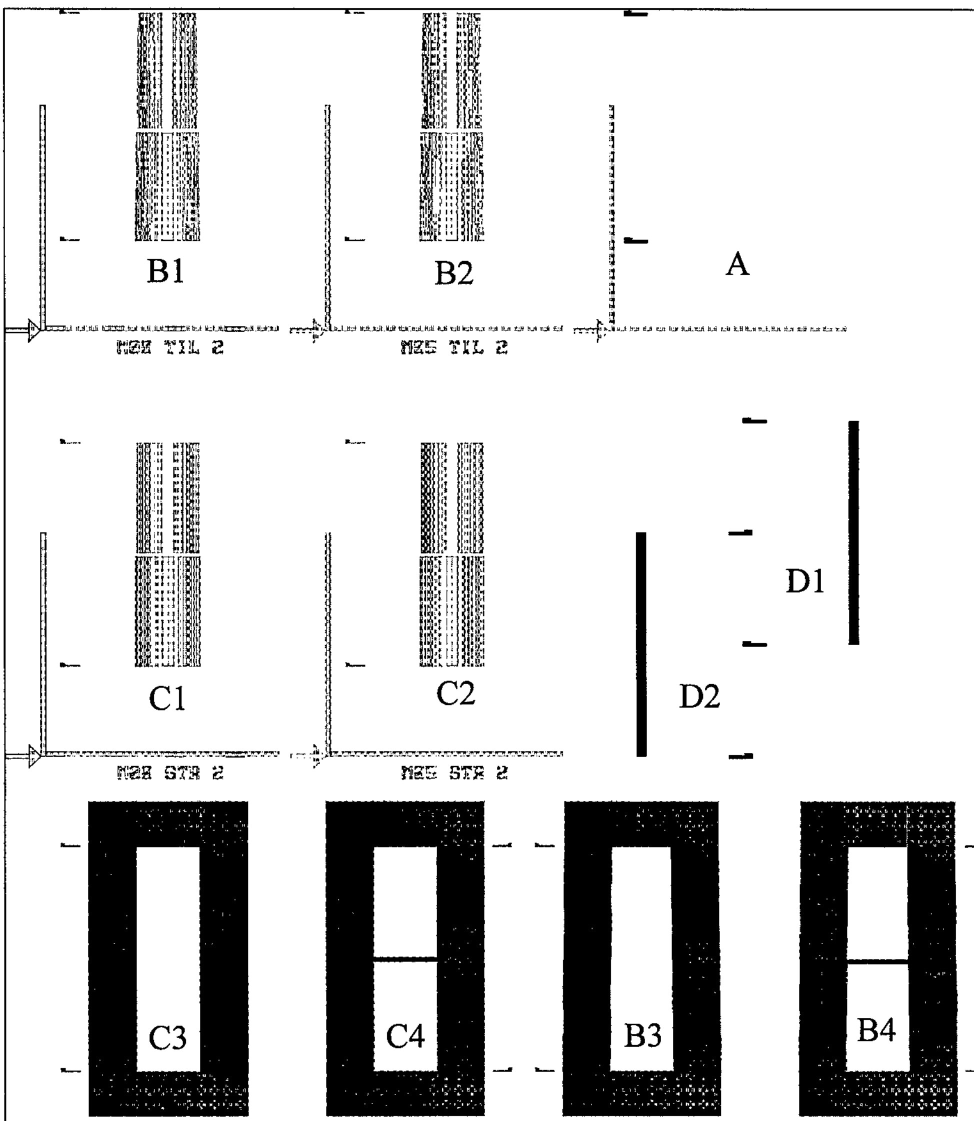

Figure 3.1 : Mask layout

Segment in Mask Layout :	For :
A	Etching alignment marks in $LiNbO_3$
B1	Resist patterning for poling. Structure : tilted; no 'undercut'
B2	Resist patterning for poling. Structure : tilted; 5μm 'undercut'
B3	Bottom electrode patterning; tilted design
B4	Top electrode patterning; tilted design
C1	Resist patterning for poling. Structure : straight; no undercut
C2	Resist patterning for poling. Structure : straight; 5 μm undercut
C3	Bottom electrode patterning; straight design
C4	Top electrode patterning; straight design
D1	Etching alignment marks in glass with respect to the groove.
D2	Mirror-image of D1

Table 3.1 : Function of individual segments of figure 3.1

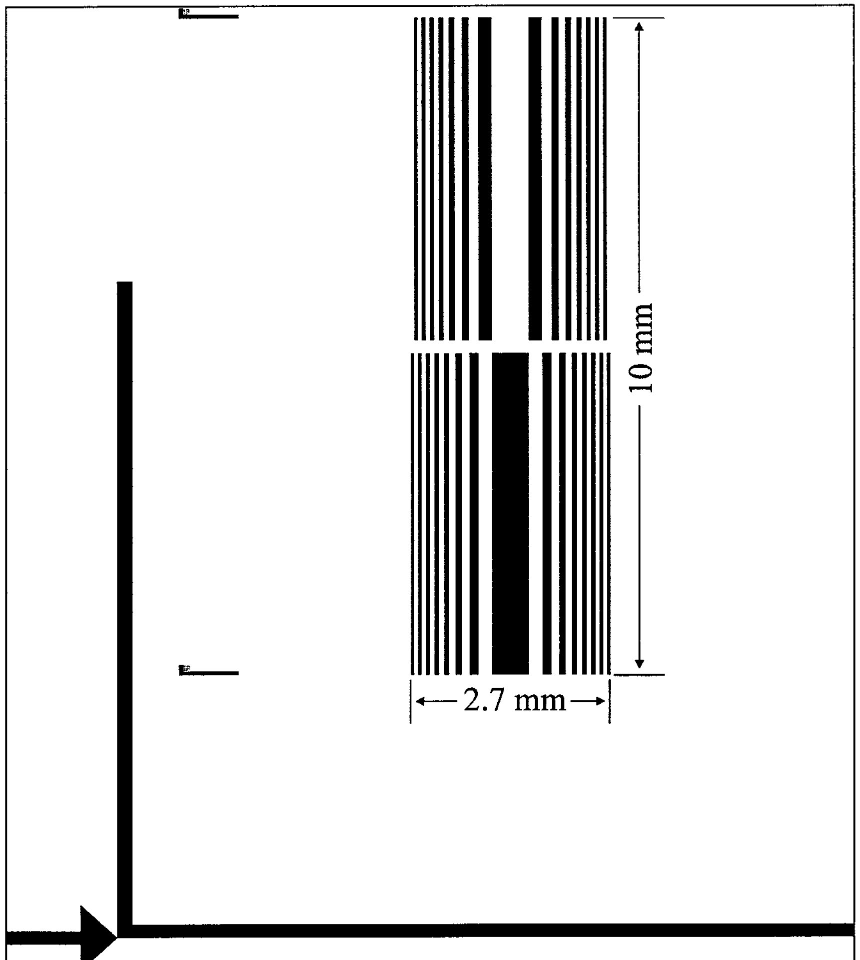

Figure 3.2 : Mask layout for phase modulator (in-line openings) (C1)

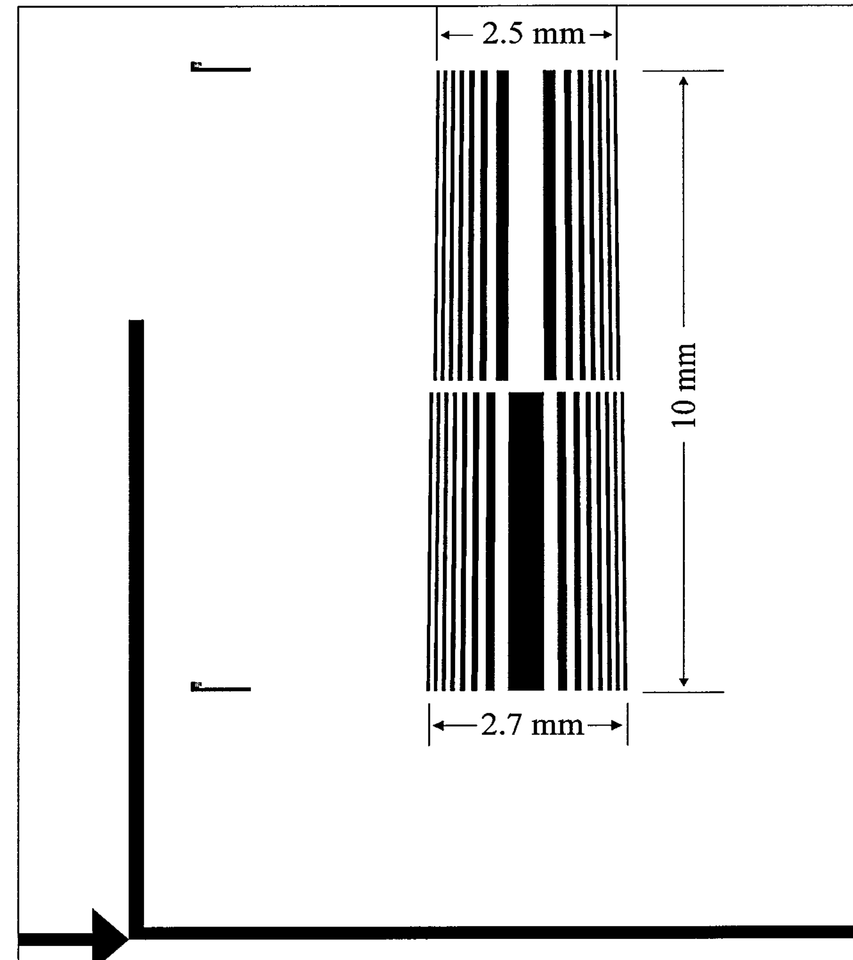

Figure 3.3 : Mask layout for amplitude modulator (tilted openings) (B1)

Figures 3.2 and 3.3 show the respective segments C1 and B1 of the mask-layout magnified and their actual dimensions. The segments consist of 2 partitions of equal size, separated by a gap of 200 μm. Each of the partitions has an inverted pattern with respect to the other one facilitating the connection of the two halves in series to double the radiation resistance and so make the device easier to match. Segment C1 has line openings which are to be parallel to the crystal's *y*-axis, thus forming a uniform focal length, whereas segment B1 has line openings to be slightly tilted with respect to the crystal's *y*-axis, forming a slanted focal length along the transducer.
In addition, in order to accommodate for some expected inverted-domain broadening - spreading underneath the electrically insulator – the segments C2 and B2 have been designed, which are identical to the respective segments C1 and B1, except that the electrode openings have intentionally been made smaller, each side by 5 μm.
The difference in the mask-layout between these two sets is illustrated in Fig. 3.4 and 3.5. Figure 3.4 shows a magnification around the centre of segment C1 having the edges of both partitions inline, whereas Fig. 3.5 shows the same for segment C2 with reduced openings, clearly visible with respect to Fig. 3.4.

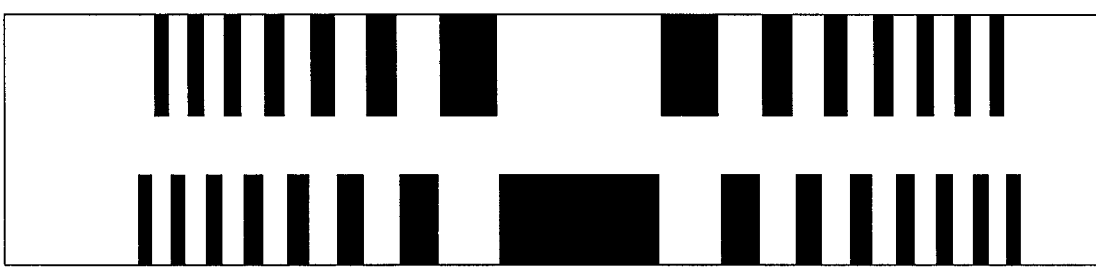

Figure 3.4 : 0 μm offset (C1)

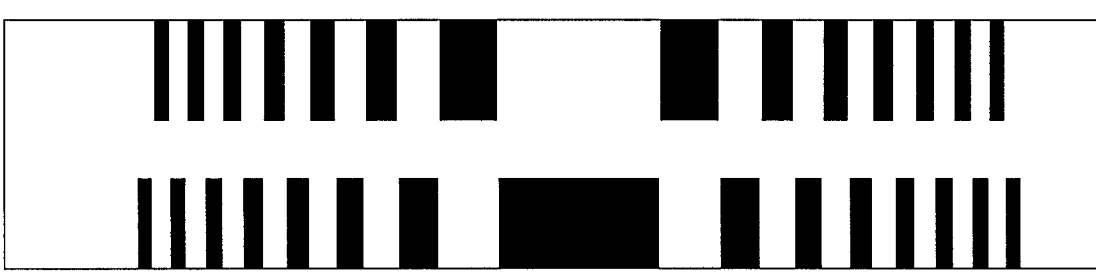

Figure 3.5: 5 μm offset (C2)

3.3 Alignment marks

Figures 3.6 and 3.7 show a RIBE-etched alignment mark in $LiNbO_3$ and its dimensions. The coarse pattern is used as orientation whereas the detail of the pattern in Fig. 3.6, which is shown magnified in Fig. 3.7, is used for the fine alignment. The squared alignment marks for fine alignment on the segments for the poling and electrode patterns are 1 μm and

2 μm smaller which enables accuracy in alignment down to 500 nm with the available mask-aligner.

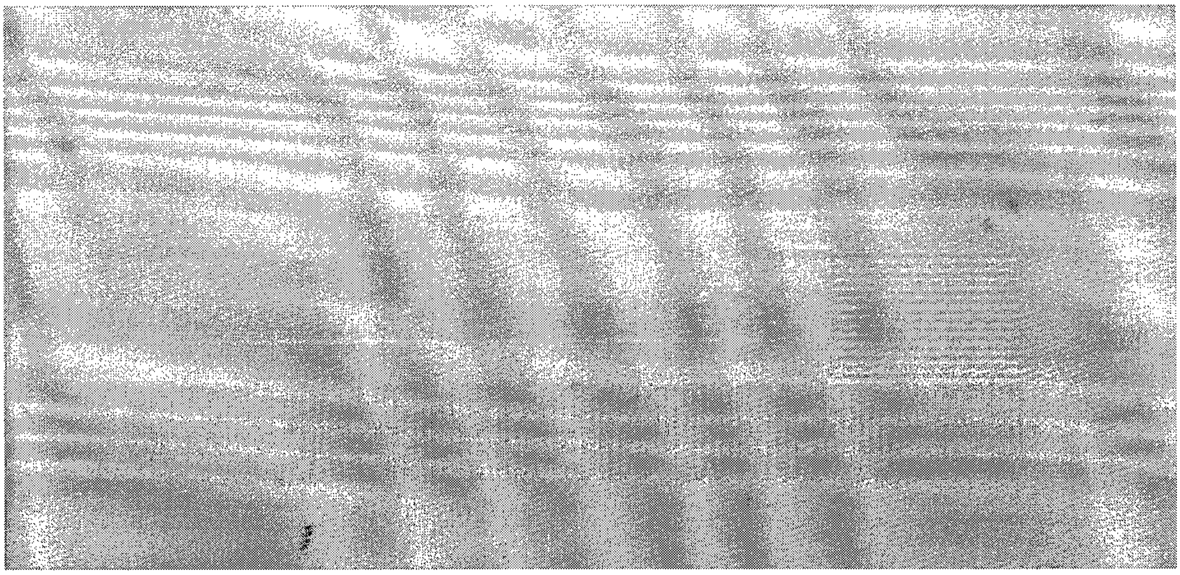

Figure 3.6 : RIBE-etched alignment mark in $LiNbO_3$

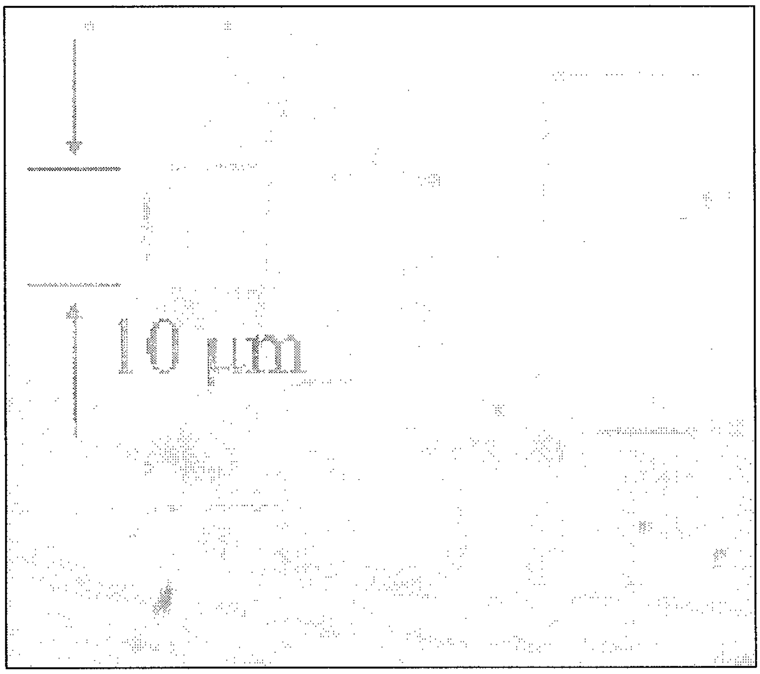

Figure 3.7 : Magnified part of alignment mark used for high resolution alignment

3.4 Experimental details of poling

The poling was carried out using a time-varying electric field under the control of a computer. The field was ramped up to a few hundred volts below the coercive field, and then ramped up to a value which exceeded the coercive field of the material, the current flowing in this second phase was monitored and integrated until the amount of charge appropriate to the equivalent surface charge of the exposed areas had flowed. Liquid electrodes were used to form the electrical connections, as shown in figure 3.8(a). Figure 3.8(b) shows schematically the fringing field, which tends to cause domain broadening unless the mask is designed to compensate for this effect.

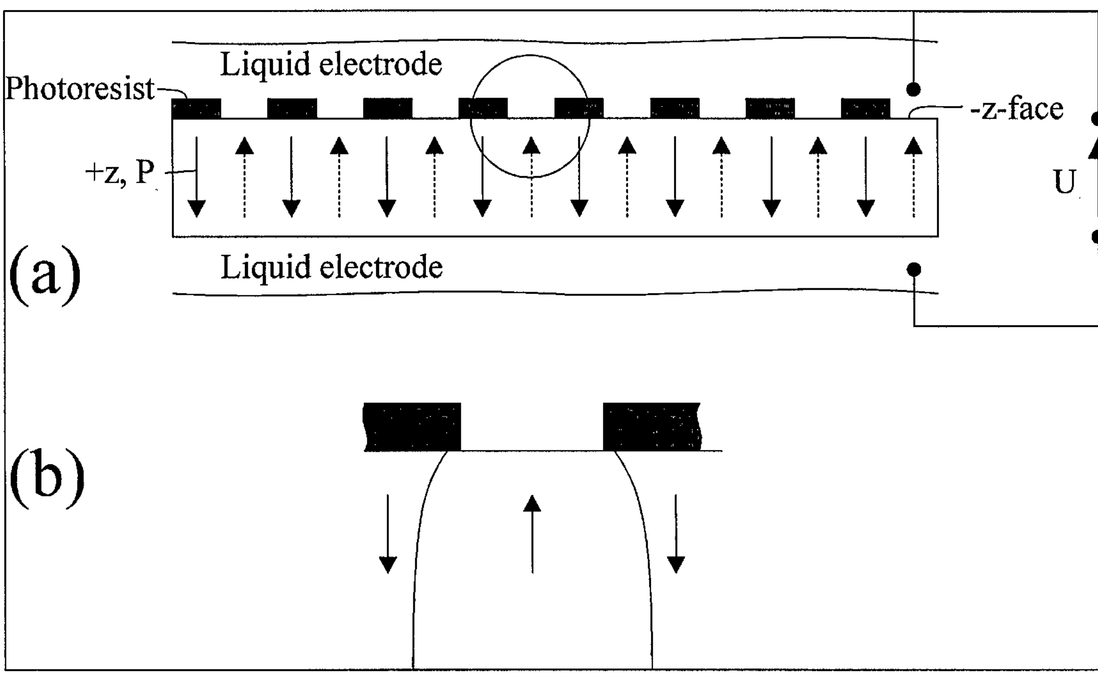

Figure 3.8 : (a) Arrangement for electric field poling using liquid electrodes; (b) illustration of the domain broadening

3.5 Results of poling

The poled samples are shown in figures 3.9-3.13, these photographs were taken using polarised light, the stress-induced birefringence in the neighbourhood of the domain walls is responsible for the contrast. It can be seen from figure 3.9 that there is some over-poling in the upper left corner, but otherwise we were very pleased with the results. A number of "pinholes" can be seen randomly distributed over all of the pictures, these are regions of inverted c-axis due to spurious "needle-shaped" domains that appear to be associated with crystal defects. These will not seriously affect the operation of the device. We found that the domains followed faithfully our mask pattern, which was inclined slightly to the y-axis by design, this being to produce a tilted focal line. We had hoped that this would be the case, but this had not been tried before, and were not 100% sure how it would behave.

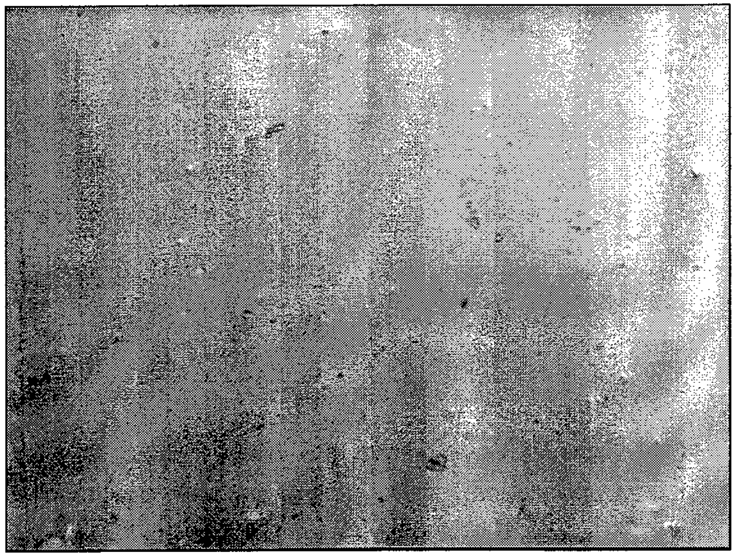

Figure 3.9 : Upper left corner

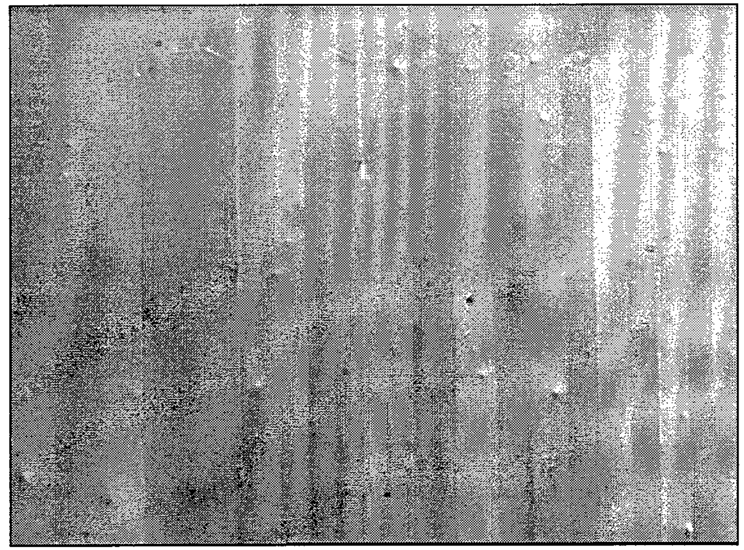

Figure 3.10 : Upper right corner

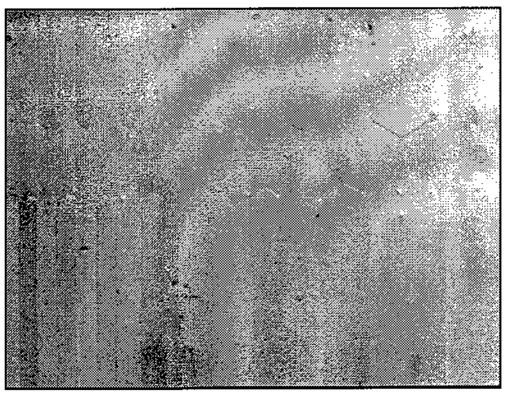

Figure 3.11 : Centre left

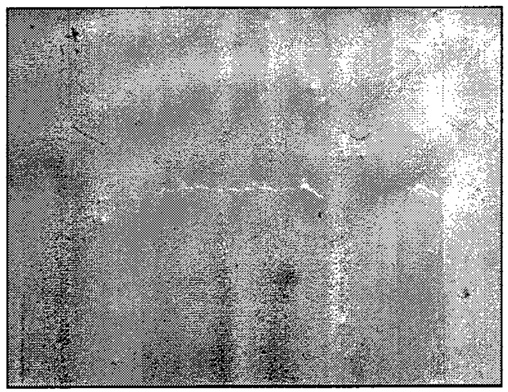

Figure 3.12 : Centre

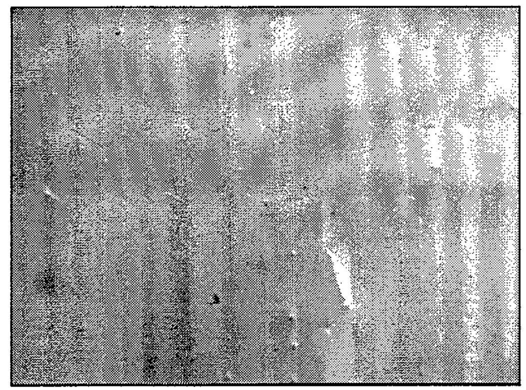

Figure 3.13 : Centre right

3.6 Design details

If the tilt angle is 3.15^{O}, because the device was specified to be 10 mm long, the focal length must change by 10mm x $\tan(3.15^{O})$ = 0.55 mm over the length of the device. If the focal length at one end is reduced from 4 mm to 3.45 mm, this will be correct to a first approximation.

In equation (1.1), therefore, $r_n = r_n(x)$ and $f = f(x)$ with $f(x)=3.45+0.055x$ ($0 \le x \le$ 10mm), and r_n is clearly not going to vary in a strictly linear fashion with x. Because of the way that f enters into the expression for r_n, we would expect the non-linearity to be most apparent for small values of n, i.e. the large low order stripes near the centre, with the worst "curvature" occurring for n=1. Figure 3.14 shows the worst case errors when a linear approximation is taken. The linear approximation greatly simplifies the mask design process, and it can be seen that the errors are negligible in the case considered here. In fact the errors in the various stripes do not vary very much, so figure 3.14 is representative.

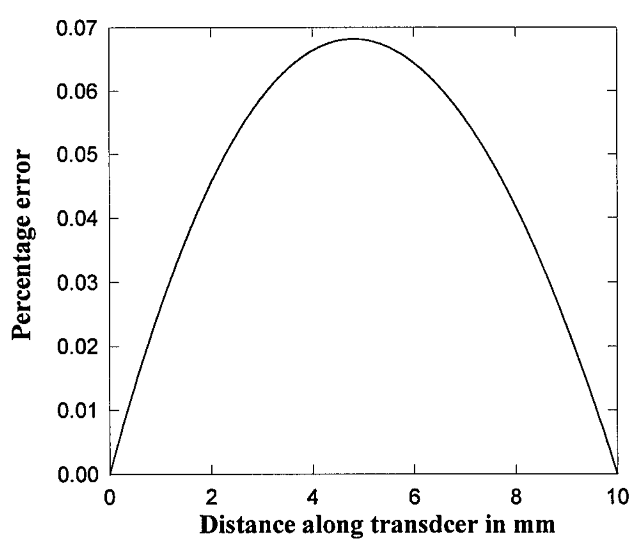

Figure 3.14 : Errors when taking a linear approximation to actual variation of stripe width with distance along transducer.

Table 3.2 shows the left-hand and right-hand positions of the regions, assuming that the device is 10mm in length. The positions shown here will ensure that the focal line is tilted by the angle of 3.15^{O} as required. The left and the corresponding right-hand dimensions corresponding to a particular value of n are joined by straight lines.

1	246.72615	229.15408
2	427.74774	397.34308
3	552.74298	513.53070
4	654.63251	608.28308
5	742.98389	690.48193
6	822.17316	764.18878
7	894.63660	831.66461
8	961.89545	894.32092
9	1024.97485	953.10864
10	1084.60425	1008.70441
11	1141.32446	1061.60986
12	1195.54968	1112.20898
13	1247.60535	1160.80322
14	1297.75232	1207.63477
15	1346.20422	1252.90137

Table 3.2: left & right hand positions of the domain boundaries in microns.

The transducer can still be divided into two regions. The two rectangular top electrodes need to have a small gap, of the order of 0.2 mm (not critical) between them. A separate mask was used to produce the top electrode pattern.

In addition to the tilted transducer which was the objective for this project, we have produced a simple pattern of parallel domain inverted regions, with dimensions of the poled regions corresponding to the first two columns of table 3.2 only. This device produces a focal line at which we plan to position an optical fibre, in order to produce a simple phase modulator. The purpose of this is to simply gain experience with the manipulation of the devices, while removing the uncertainty associated with the production of tilted regions. As explained, it turned out that the production of these tilted regions caused no problems, but the masks were designed so as to be capable of generating both types of transducer.

3.7 Conclusions

In this section we have presented details of the mask design and the arrangements used to ensure that the correct alignment can be obtained between the various components in the final device. In addition the poling process used has been described, and the experimental results appear to be of good quality.

It appears feasible that the particular form of the domains, tilted with respect to the y-axis of the crystal causes no problems.

We designed photolithographic masks which could also be able to produce simple phase modulators, as a "control" and because another type of interesting component could thus be produced with relatively little extra effort.

4 Transducer alignment and bonding

4.1 Methodology used to obtain alignment

During the production of acousto-optic modulators, we were presented with the problem of aligning a transducer with marks that are on the opposite side of a glass block. Since the accuracy of alignment must be in the order of 10 μm, this must be carried out under a microscope. Most microscopes do not have a focussing slide that is absolutely parallel with the centre line of the optics, which is the root of the difficulties. We therefore had to develop a scheme by which the alignment could be accurately assessed, and tools with which the alignment could be corrected prior to bonding. This assembly had to be suitable for transfer into the heated press that was used to cure the bonding adhesive.

4.1.1 Geometry of the problem

The transducer is mounted on a substrate consisting of a block of BK7, 10mmx15mmx4.23mm thick. Alignment marks have been made on the bottom of the glass block and the bottom of the transducer. The focussing stage of the microscope used to view the alignment is not expected to be parallel to the centre-line of the lenses, nor is the glass initially assumed to be perpendicular to either of these lines. It is arranged that the transducer and block can be freely rotated in the x-y plane, and that the inclination of the glass with respect to the focussing stage can also be adjusted. All alignments are carried out as close as possible to the centre line of the optics. The arrangement is shown in figure 4.1 below.

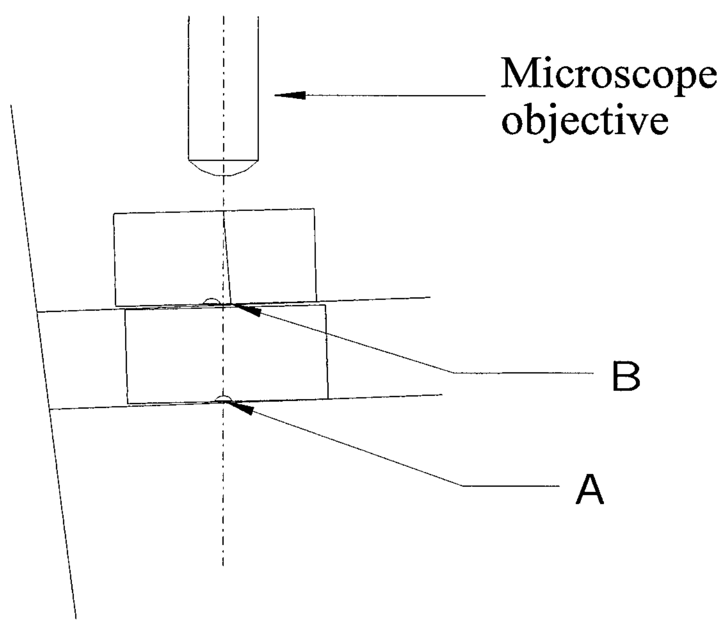

Figure 4.1

Point A shows the desired position of the glass for a given transducer position on the centre-line of the optical axis, the transducer omitted here for clarity. When the glass block is brought up to a position where the focus is at its base, we can immediately see two sources of error. First there is the error in the alignment of the focussing stage with the optical axis, since they are not parallel. This is given by $\Delta x_1 = d \sin\theta$, where d is the depth of the glass and θ is the angle of misalignment. A further error is given by the fact that the glass block is not perpendicular to the optical axis, which is given by $\Delta x_2 = d \sin\alpha / n$, where α is the angle between the glass block and the optical axis, and n is the refractive index of the glass.

Solution

We rotate the glass through half a turn and recheck this alignment. The error from Δx_2 immediately becomes apparent, and is minimised by levelling the sample. After several checks the error is reduced to an apparent deviation in position of less than 6 μm.

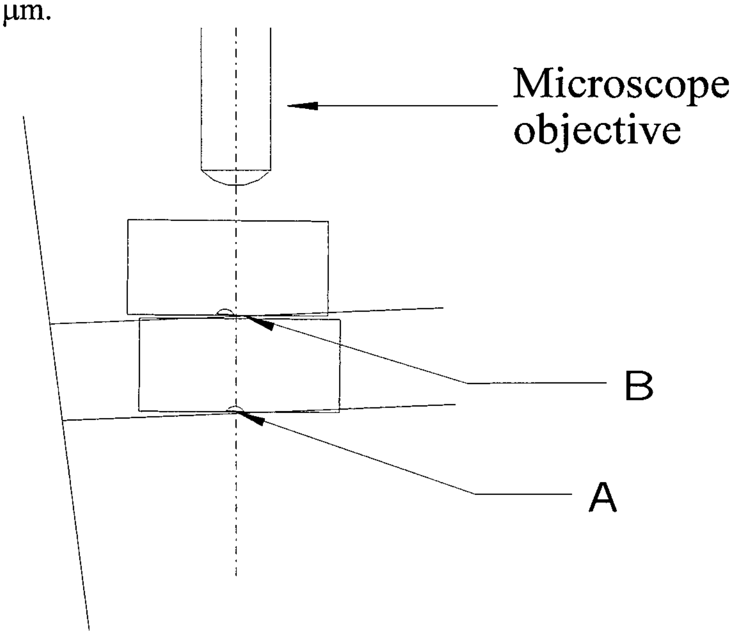

Figure 4.2

We are now left with a misalignment given purely by the non-parallel movement of the focussing stage. However, if the sample is repeatedly rotated and readjusted so that the apparent misalignment is the same in both positions, it is clear that the actual position will lie half way between two apparent positions. This means that the transducer position will be measured to a greater accuracy than the resolution of the microscope.

The rotation stage of the jig was found to have an angular deviation of 0.018 degrees. The error in alignment through a 4.23 mm BK7 block is therefore less than 2 microns.

Since the microscope resolution, using a X10 long working distance objective lens, is 7 μm, we can estimate that the alignment is carried out to an accuracy of 4 μm.

4.2 The substrate-transducer alignment jig

A jig was produced in order to carry out the alignment. Its design criteria included the following:

1. Glass block must be securely anchored.
2. It must be possible to accurately position the transducer in a single plane.
3. It must be possible to rotate the transducer in a single plane.
4. The jig must be mounted so that it can be rotated.
5. It must be possible to adjust the plane of rotation of the jig.
6. It must be possible to transfer the jig to a heated press without disturbing the transducer position.

In order to meet these criteria the jig was designed so that the glass block is placed in a recess and secured by two spring-loaded push rods. The transducer is then placed on top of the glass block, with bonding adhesive in place. Its position can be adjusted by three pushrods, driven by adjusting screws. These pushrods are opposed by two spring-loaded pushrods.

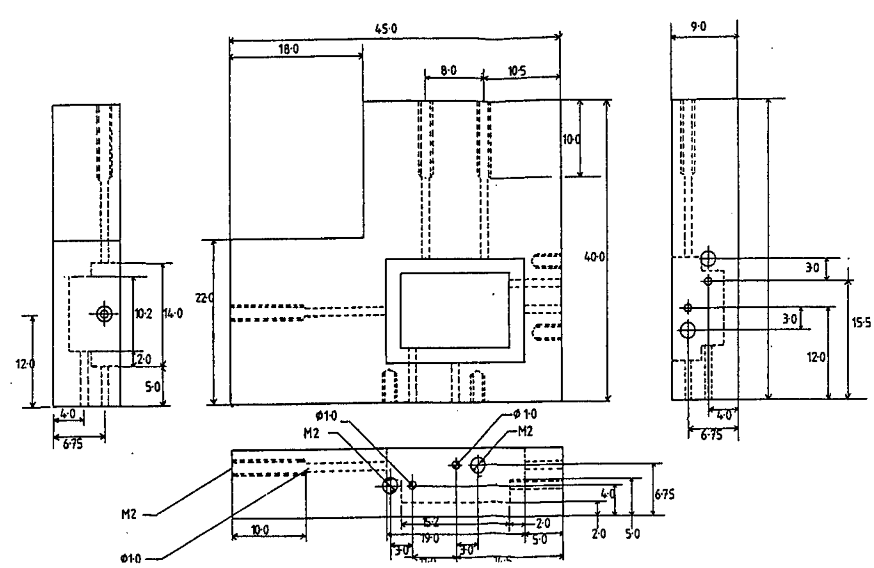

Figure 4.3 : Transducer alignment jig, main body

The body of the jig was mounted onto a turntable running on three ball bearings. The turntable has adjustable feet so that the angle can be adjusted perpendicular to the optical axis. One final adjustment to the design was the inclusion of two windows in the base of the jig, so that the alignment marks could be uplit during alignment in the microscope.

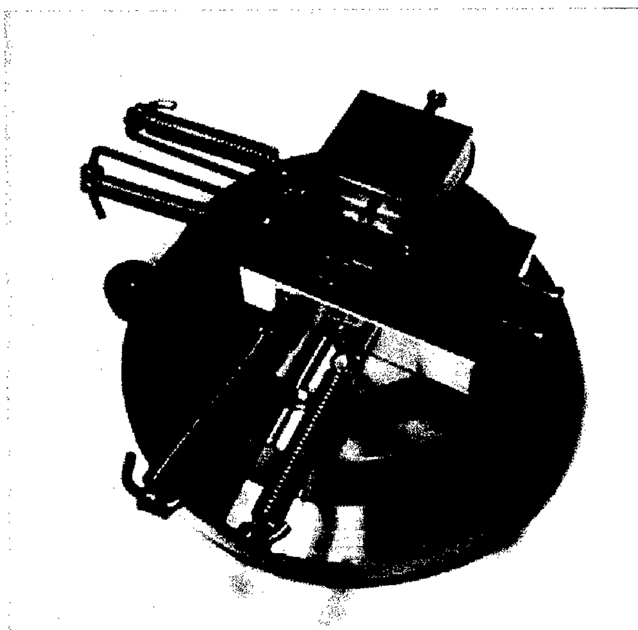

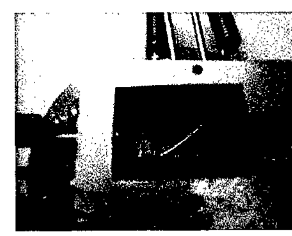

Figure 4.4: Alignment jig on turntable

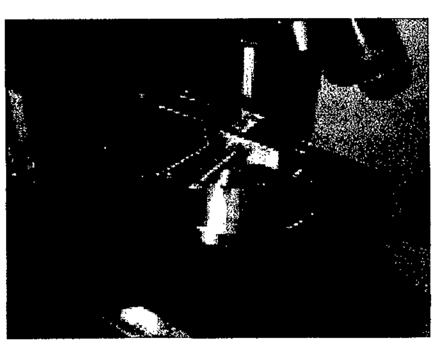

Figure 4.5: Alignment jig under microscope

The jig is rather difficult to use, but with practise reasonably repeatable results were obtained. It is very important to ensure good finish on the edges of the transducer to avoid damage from the positioning push-rods, but the stability of the jig at up to 150 Celsius has been verified.

4.3 The compression bonding jig

A compression bonding jig was produced for the project. The bottom jaw of the press is mounted on bearings so that it is self levelling. Additionally both jaws are insulated with a ceramic material so that the jaws (and anything between them) may be heated.

The press is fitted with a 100 Watt heater element and thermocouple probe position. Samples can be heated to 150 Celsius in around 20 minutes, although a slower rate is generally preferred.

The press is loaded by placing weights on the top tray, to a maximum of around 60 N. With the devices built for this project this equates to a pressure of about 400 kPa.

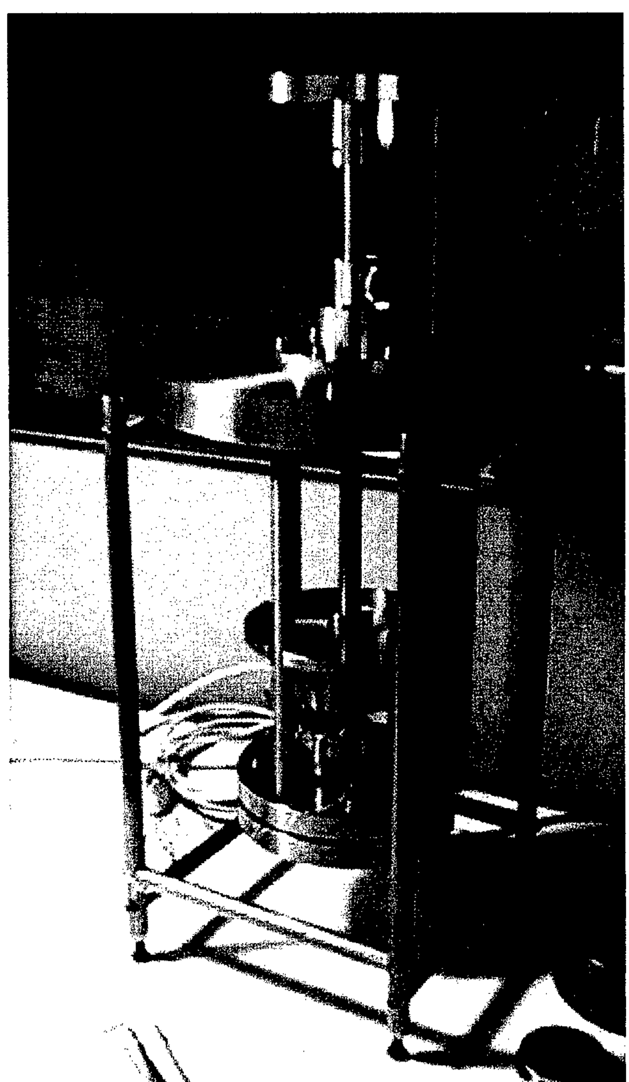

Figure 4.6: Compression bonding Jig

4.4 Choice of epoxy

It was decided reasonably early in the project to use epoxy resin to bond the transducer to the glass block. The rationale for this was as following:

1. Adhesive must be transparent to allow alignment.
2. Adhesive must be reasonably hard.
3. High temperature capability is of benefit.
4. Adhesive must not dissolve in any chemicals used for cleaning or later manufacturing processes.
5. Must be possible to place in thin layers.

Other adhesives that were considered included anaerobic adhesives, which fall down on points 3 and 4, and Indium solder, which fails at point 1. We have considered devising a methodology in which Indium solder could be used, as it has excellent acoustic properties for this purpose.

Initially it was felt that it would be of benefit to spin coat uncured adhesive onto one of the surfaces to be joined, but since epoxy resin mixtures are reasonably viscous with quite high surface tension this proved to be unsuccessful. The best method proved to be to put a small drop of the adhesive onto each face to be joined, and then place them together, allowing the capillary action of the glue to slowly expel any included air.

Most early experiments were carried out using Epo-Tek 353ND, but this proved to be rather too viscous to form a bond less than 10 μm thick. Further experiments were then carried out using Epo-Tek 360, which has a very low viscosity at 400 cps. It has been found that at a pressure of 200 kPa a glue line of thickness 1.5 μm can be formed with this adhesive.

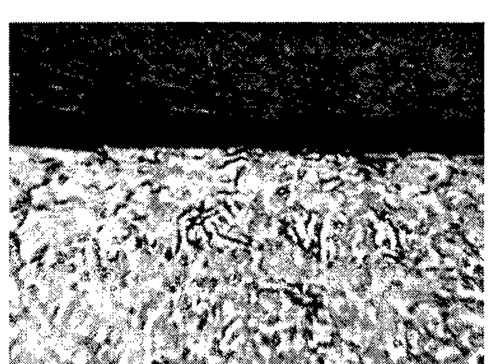

Figure 4.7: Section through glue line following recipe below:
Glue line is approximately 1.5 μm thick

The current recipe for gluing is as follows:

Mix Epo-Tek 360 parts A and B @ 10:1, accurately measured by weight.

Allow to de-aerate in vacuum desiccator, 20 minutes

Clean samples for gluing, in cleanroom, and inspect for dust/contamination greater than 100 nm in structure.

Apply glue to both faces and allow joint to form.

Place in alignment jig and carry out alignment.

Place in compression bonder and allow to settle under light pressure.

Slowly increase pressure to 200 kPa and allow to settle for 10 minutes.

Heat press to 150 Celsius over 30 minutes, hold for 2 minutes, cool to room temperature over 1 hour.

We have recently found shortcomings in this method, the biggest problem being the 1.4% shrinkage that even the most stable epoxies exhibit on curing. The problem manifests itself as a tendency for the Lithium Niobate transducers to crack during later processes. We are currently addressing this problem using a lower temperature curing epoxy - Epo-Tek 301-2 – and hope that will ensure transducers survive the whole of the manufacturing process.

4.5 Results obtained after polishing

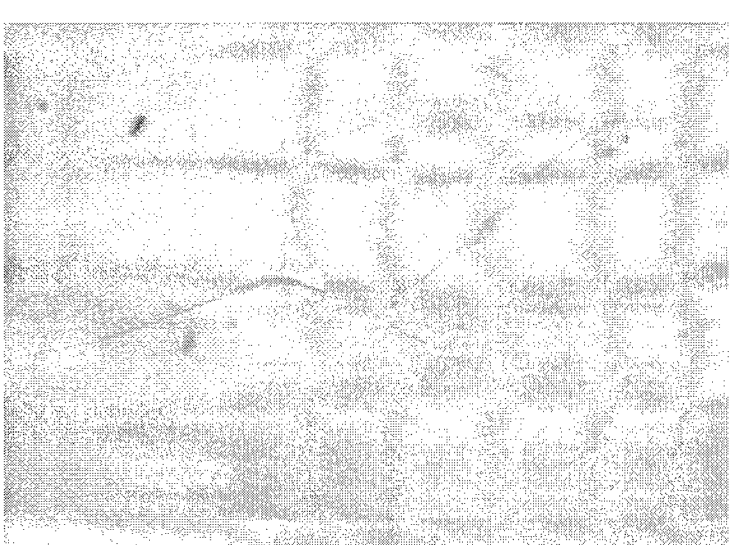

Figure 4.8: Cracking of transducer

After bonding the transducer onto the substrate, it must be polished down to the design thickness, which is close to 20μm. We are currently experiencing problems of transducers cracking during the polishing operation, as stated in the previous section, and as shown in figure 4.8. We are actively seeking ways to prevent this happening, it seems to be associated with voids, probably caused by the epoxy out-gassing during the relatively high temperature curing operation. We are currently using a vacuum desiccator to remove dissolved air prior to bonding, and have selected a lower temperature epoxy, and we believe that the problem will be solved by these modifications.

4.6 Transducer thickness measurement

The transducer lapping and polishing was done on a "Logitech" polisher, after the polishing jig with attached substrate/transducer was adjusted so as to be parallel to the reference surface of the jig. It is necessary to be able to polish down to the design thickness, so an optical system was evolves in which the jig, with the substrate still attached, could be inspected at various stages in the polishing process. This was done using a motor-driven precision rotation stage on which the jig was mounted so that the angle of

1

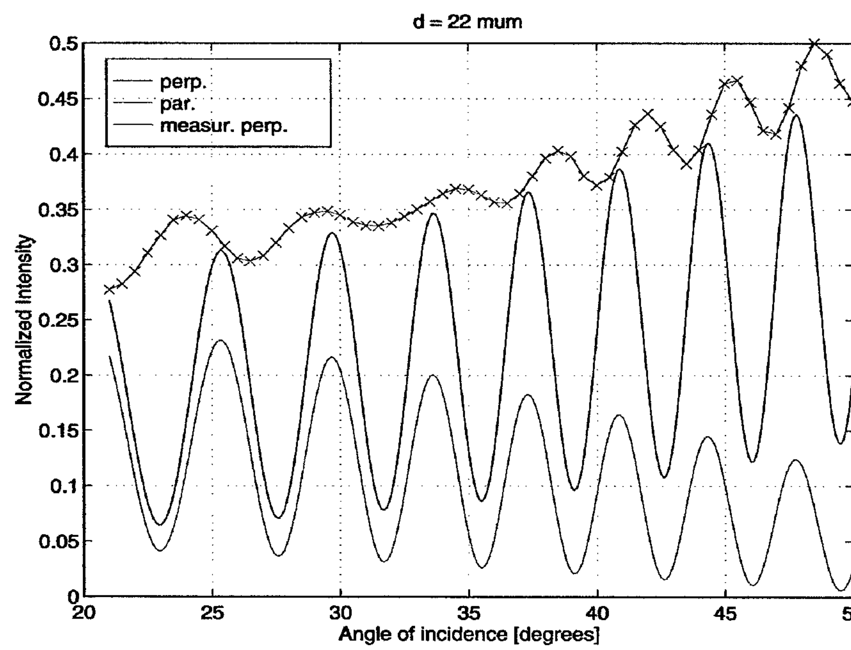

Figure 4.9: Theoretical and experimental results for transducer thickness measuring apparatus

incidence of a HeNe laser beam could be varied. After multiple reflections in the relatively high index material of the transducer, the beam was incident on a photodiode, the current vs. angle is shown in figure 4.9. The information we require is contained in the frequency of oscillations, the loss of visibility in the experimental curve is due to mechanical misalignments occurring during rotation, and is not important. We have found that this inspection method is vital in the manufacture of these devices, as the mechanical tolerances in the transducer thickness are only a few percent.

4.7 Conclusions

This section has concentrated on the problems of transducer alignment, bonding, polishing and thickness measurement, and how they have been overcome. We have had to build a number of specialised pieces of apparatus in order to do this. We are generally very pleased with the results obtained, but we are at the time of writing this report, still experiencing problems due to the cracking of the transducers during polishing. We are currently trying to solve these problems.

5 Fibre bonding

5.1 Procedure used to bond fibre into groove

This procedure has been used before but not yet used on this project. We have obtained a supply of aluminium-jacketed telecomm fibre, and the outer diameter of this is 175 μm, i.e. the aluminium is 25μm thick. The specific acoustic impedance of aluminium is similar to that of BK7 (see table 1.1) , and so we do not anticipate problems at this stage. In the past we have plated a thin film of nickel over the aluminium and indium soldered it into the groove, in this case the groove will be pre-coated with Cr/Au to facilitate adhesion and the formation of an acoustic joint of high quality. If we switch to an epoxy having a lower cure temperature in order to try and solve the cracking problem, we will indium solder the fibre into the groove *before* the transducer polishing operation.

6 Personnel involved

Besides the input of Chris Pannell (Sensormetrics Ltd and the University of Kent), there have been two people involved:

Liam Humberstone is a PhD student, and he has been involved full-time since August of 1999, when the post became vacant after the previous student, Mr Arnold, left prematurely. Mr Humberstone will be studying for three years for his PhD, He is a DTI CASE student, funded through Sensormetrics Ltd.

Harald Gnewuch has devoted much time to this project and has been responsible for most to the production of photolithographic masks, and poling. He is employed on a consultancy basis for this project. He too, will be available for direct input into this work which will continue past the project end-date as it now forms the subject material of Mr Humberstone's PhD.

7 Overall conclusions

This project is for the construction and investigation of the type of fibre-optic amplitude modulator which operates by coupling from the fundamental guided mode of a telecomm fibre operating in the 1.5 μm region of the spectrum, to cladding modes. The initial phases considered of exploring the possibilities offered by several different methods of construction, and the detailed design of the acoustic transducer. During this phase, a number of mathematical models were set up, including the prediction of the form of the focal region and the "figure of merit" afforded by the use of domain-inverted transducer technology.

We found that the figure of merit which we defined as (the acoustic intensity in the focal region)/(the acoustic intensity of an equivalent planar transducer) was of the order of 9, but in practice the presence of acoustic aberrations may reduce this to 6 or 7. In addition to this, we developed a computer programme for the prediction of the electrical impedance of the device as a function of frequency, for a variety of bond thickness and materials. We found that using epoxy rather than indium compression bonding, we could guarantee an electrical radiation resistance of the order of 10Ω per section, and as there are two sections connected in series this rises to 20Ω, which is a good figure for matching considering the large size of the transducer array (2.7mmx10mm) for this frequency (196 MHz).

We have modelled the epoxy bond as a lossy acoustic transmission line, and the graph of figure 1.4 summarises the predicted behaviour, and indicates that for thin bonds, of the order 2 μm or thinner, absorption is not a major problem. The down-side of the use of epoxy to offer increased radiation resistance, is that the bandwidth of the transducer is narrowed, and this places additional problems in the operation of transducer lapping/polishing, the plate thickness must be controlled to a few percent. However, using the optical arrangement of section 4.6 we can achieve this. Other problems which had to be surmounted include the alignment of the transducer focal line with the optical fibre, we have constructed a number of mechanical fixtures to enable this to be done, and demonstrated that they work to the tolerances required.

We are currently experiencing problems of transducer cracking during the polishing operation, but we feel that this is not a fundamental issue, but rather an engineering problem which will disappear when we have found the correct procedure (i.e. which epoxy, curing temperature, bond pressure, polishing parameters), to use. This work will continue during the course of Mr Humberstone's PhD project, and all results and devices will be made available to Dr Szczepanek.